Theoretical study of cellobiose hydrolysis to glucose in ionic liquids

Yoshifumi Nishimura [a,b], Daisuke Yokogawa [a,c,*], Stephan Irle [a,c,*]

[a] Department of Chemistry, Graduate School of Science, Nagoya University, Furo-cho, Chikusa-ku, Nagoya 464-8602, Japan
[b] Department of Applied Chemistry and Institute of Molecular Science, National Chiao Tung University, 1001 Ta-Hsueh Road, Hsinchu 30010, Taiwan
[c] Institute of Transformative Bio-Molecules (WPI-ITbM), Nagoya University, Furo-cho, Chikusa-ku, Nagoya 464-8602, Japan

ARTICLE INFO

ABSTRACT

The S_N1-type hydrolysis reaction of cellobiose in ionic liquids (ILs) was theoretically investigated. First principles and *ab initio* quantum chemical methods were used in conjunction with the 'reference interaction site model self-consistent field with spatial electron density distribution' (RISM-SCF-SEDD) method. Reaction mechanism pathways are discussed and compared to calculations in gas phase and in aqueous solution. Analysis of solvation effects indicates strong interaction between hydrogen atoms of glucose hydroxyl groups and the anions in ILs, contributing to large stabilization of the reaction product. The calculated activation energy in ILs (24.5 kcal/mol) agrees quantitatively with the experimental value (26.5 kcal/mol).

1. Introduction

With the exhaustion of petroleum resources in sight, the importance of biomass as renewable energy resource in the production of biofuels is rapidly increasing. One of the key steps for the use of biomass is the degradation of cellulose and hemicelluloses, most abundant chemical components in biomass [1]. For yielding monosaccharides, hydrolysis treatment with mineral acids such as HCl and H_2SO_4 is commonly used, which is very simple reaction yet brings several disadvantages (e.g. corrosion of reactor [2] and further decomposition of glucose [3]). Recently, ionic liquids (ILs) have shown great promise that they could dissolve cellulose directly under relatively mild conditions (about 100 °C, 1 atm) [4]. Furthermore, efficient hydrolysis of cellulose in ILs was demonstrated in the presence of acid catalysis [5], by mixing with water [6], or with catalytic amounts of metal halides [7,8]. It is highly desirable to further develop this environmentally benign technology.

Ab initio quantum chemical calculation is ideal for understanding the details of reaction mechanisms at the atomistic level. Previously, several theoretical studies were reported on the acid-catalyzed hydrolysis of sugar related compounds in gas phase or aqueous solution [9–12]. However, the number of publications dealing with chemical reaction of sugars in ILs theoretically is very limited at present. For example, Liu and co-workers addressed the interaction of cellulose oligomers with imidazolium-based ILs

using molecular dynamics (MD) simulations with their in-house developed force field parameters [13]. The main reason for the scarcity of theoretical studies arises from the fact that the conventional quantum chemical approaches have great difficulty to manage both (i) simultaneously treating different types of solvent molecules (organic cation and organic/inorganic anion components for ILs) and (ii) describing intermolecular interactions like strong long-range Coulomb interactions and weak short-range dispersion accurately at the same time. We note that the utility of fragment molecular orbital (FMO) method [14] to ILs was introduced during the past few years [15,16].

In this work, we have studied the S_N1-type hydrolysis reaction of cellobiose into two glucose units using quantum chemical first principles and *ab initio* methods in conjunction with RISM-SCF-SEDD [17,18], which is a hybrid method between quantum chemical calculation and reference interaction site model (RISM) [19–22]. Cellobiose is the simplest molecular model for cellulose to study the hydrolysis of the glycosidic bond. The RISM-SCF-SEDD method allows to obtain valuable information about the solvation effect at an economical computational cost, owing to an analytical treatment via the RISM approach. Its successful applications to Diels-Alder [23] and S_N2-type reaction [24] in ILs indicate that this method suits well for our present purpose. We expect that exploring reaction energy profile and the role of solvents around solute molecules enhances the fundamental knowledge on such reaction processes.

2. Computational details

Geometries of all species were optimized using the B3LYP method [25,26] in combination with the 6-31+G(d) basis set [27–

* Corresponding authors at: Department of Chemistry, Graduate School of Science, Nagoya University, Furo-cho, Chikusa-ku, Nagoya 464-8602, Japan.
  E-mail addresses: d.yokogawa@chem.nagoya-u.ac.jp (D. Yokogawa), sirle@chem.nagoya-u.ac.jp (S. Irle).

29]. The nature of stationary points on the potential energy surface (PES) was characterized by carrying out harmonic vibrational frequencies in each case. At the same level, the thermal correction to Gibbs free energy at a finite temperature was computed without applying any scaling factor. Single-point energy profiles were calculated by employing spin-component-scaled second-order Møller-Plesset purterbation theory [30] with resolution-of-identity approximation [31,32] (RI-SCS-MP2) and the aug-cc-pVDZ basis set [33,34]. 1,3-Dimethylimidazolium chloride ([mmim][Cl]) was selected as a model of ILs since imidazolium-based ILs are most frequently used in experiment [4–8,35]. It was reported that the simplified [mmim]+ qualitatively reproduces general experimental trends of imidazolium cations with alkyl chains [23,24]. For comparison, two additional phases – gas phase (at a temperature of 300 K) and aqueous solution (water) – were considered. The temperature of the solvents was set to 300 K for water and 373.15 K for [mmim][Cl] in RISM-SCF-SEDD calculations. 0.033426 molecules/Å³ and 0.004871 molecules/Å³ were adopted as the density of water and [mmim][Cl], respectively. The Lennard-Jones parameters for solute and solvents were listed in Table S1 in the Supplementary material. The integral equation of RISM theory was solved using the Kovalenko-Hirata (KH) closure equation [19,20,36]. To accelerate the convergence speed of RISM-SCF-SEDD calculations, we removed the auxiliary basis functions on carbon and oxygen with the smallest exponent and expansion coefficients [18]. Geometry optimization and transition state search in gas phase were performed using the Gaussian 09 program package [37], while all other calculations were carried out using the GAMESS program package [38] with our implementation of RISM-SCF-SEDD.

3. Results and discussion

3.1. Geometry changes

Figure 1 shows our proposed reaction scheme. The hydrolysis reaction begins with the formation of complex 2 where the glycosidic oxygen of cellobiose 1 is protonated by a hydrogen-bonded hydronium cation. Next, the protonated species 3 is separated into glucose 7 and a positively charged compound 5 via transition state TS_{34} where cleavage of the glycosidic bond occurs. Here, species 3 and intermediate 4 were optimized following the intrinsic reaction coordinate (IRC). Subsequently, the anomeric position of compound 5 is attacked by one water molecule. Finally, another water molecule acts to remove a proton from species 6, producing the second glucose unit 7. It is noteworthy that Liang and co-workers have reported a similar step-wise reaction based on Car-Parrinello MD-based metadynamics simulations with inclusion of associated solvent molecules in aqueous acid [12]. They noted that the concerted hydrolysis process is not significantly unfavorable [12].

The optimized structures for the phases – gas phase, water, and IL – are illustrated in Figure 2. All Cartesian coordinates are included in Table S2 in the Supplementary material. Complex 2 indicates the establishment of three intramolecular hydrogen bonds in gas phase, but one of them is missing in solution. Both glycosidic bonds in 2 are elongated by ∼0.1 Å after protonation of 1. One glycosidic bond is further elongated by 0.1 Å in going from 3 to TS_{34} whereas the other decreases to 1.49–1.50 Å in TS_{34}. We roughly consider a distance larger than 2.4 Å in the pre-dissociation complex 4 as evidence for C–O bond breaking. Note that one intermolecular hydrogen bond (1.72–1.75 Å) between the two glucose units still remains intact in 4. The oxonium form of 5 presented in Figure 1 is deduced from two features at the B3LYP/6-31+G(d) level in gas phase: (i) the C–O Wiberg bond index [39] involving the intracyclic oxygen is 1.54 in 5, indicating at least partial double-bond character, and (ii) the natural atomic charge on the glucose oxygen involved in the former glycosidic bond becomes more negative (−0.37 for 5 and −0.60 for 7, whereas it was –0.58 and –0.62 in 1). In 6, a water molecule attacks the carbon atom of the intracyclic C=O double bond of 5, which leads to elongation of the C–O bond by approximately 0.1 Å. The newly formed C–O single bond in the gas phase is about 0.1 Å longer than predicted in water and
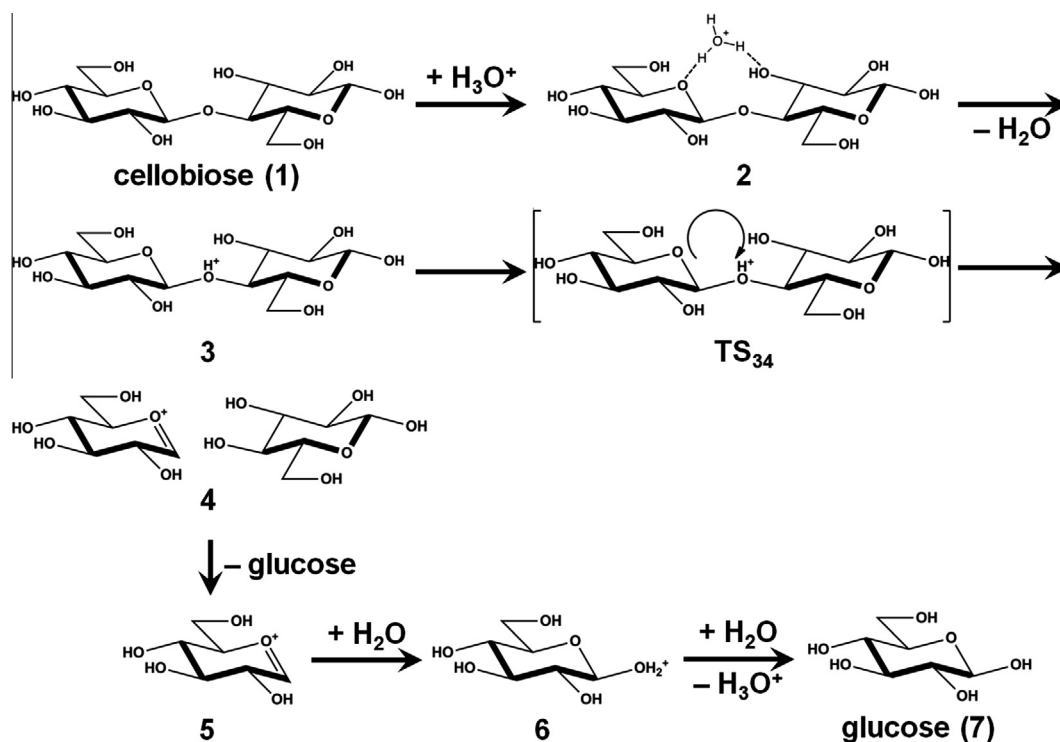

Figure 1. Investigated S_N1-type hydrolysis reaction scheme from cellobiose 1 to glucose 7.
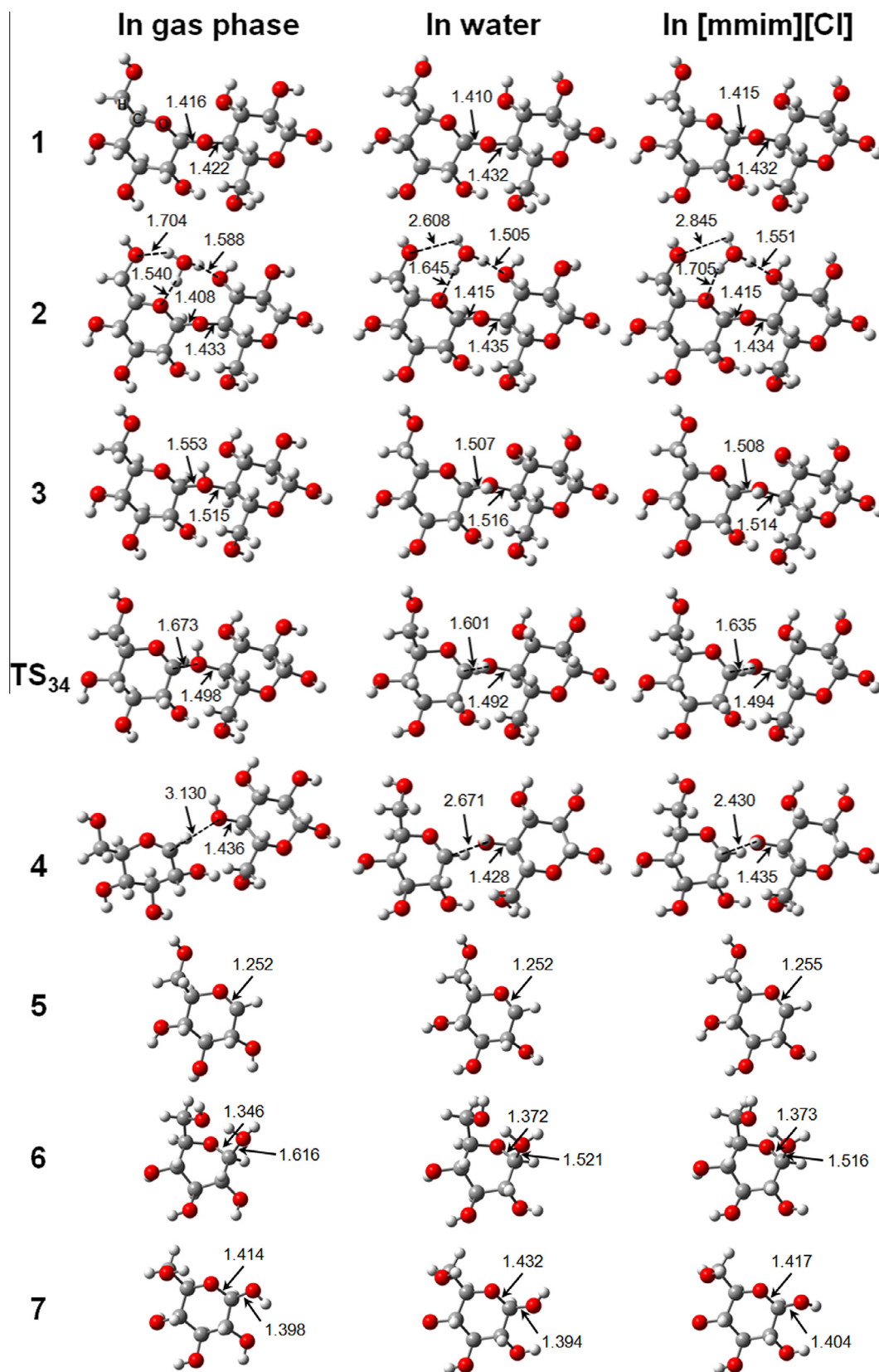
Figure 2. B3LYP/6-31+G(d) optimized geometries in gas phase (left), in water (center) and in [mmim][Cl] (right) for species **1–7** and **TS₃₄**. The selected C–O bond lengths are given in units of Angstrom.

[mmim][Cl]. One intramolecular hydrogen bond seems to exist in **6** according to the distance between a proton of the $-OH_2^+$ group and the oxygen atom in the CH_2OH group (O–O distance is about 2.5 Å).
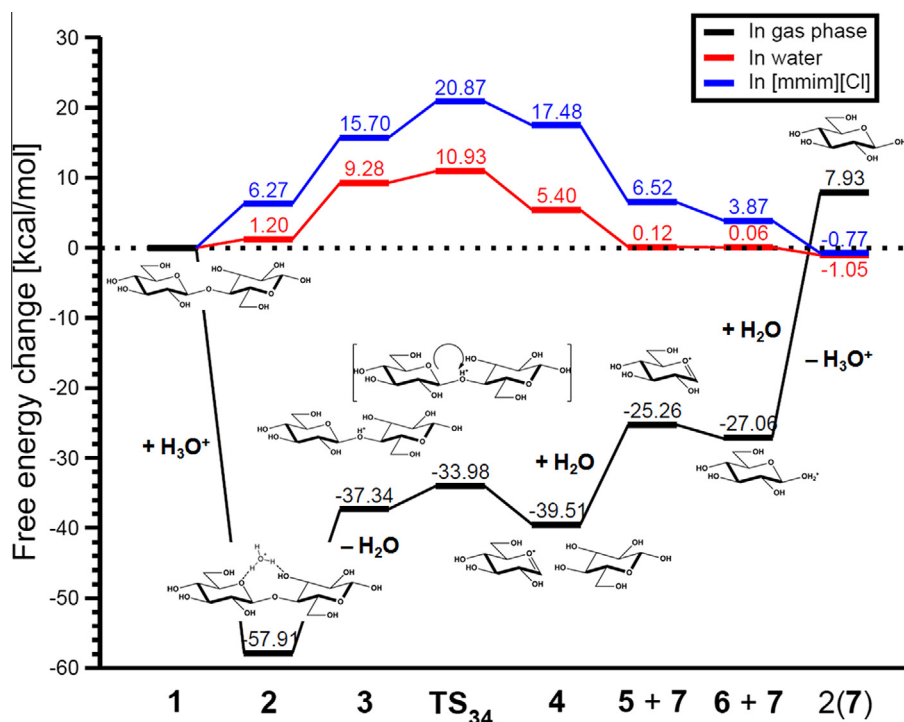
Figure 3. RI-SCS-MP2/aug-cc-pVDZ//B3LYP/6-31+G(d) free energy changes in gas phase (black), in water (red), and in [mmim][Cl] (blue). (For interpretation of the references to colour in this figure legend, the reader is referred to the web version of this article.)

3.2. Free energy changes

The free energy changes along the reaction path of Figure 1 for the three phases are given in Figure 3. In gas phase, the strong interaction between **1** and the hydronium cation contributes to large stabilization of complex **2** and the reaction is energetically favored until the final deprotonation. However, this proton removal from **6** requires 35.0 kcal/mol energy, making the overall reaction endothermic by 7.9 kcal/mol. The reason for this large energy requirement becomes apparent by inspecting the atomic charge difference between cation and neutral molecule. Natural population analysis demonstrates that the positive charge in **6** is completely delocalized over the entire sugar ring (see details in Figure 4). This suggests that stabilizing the leaving hydronium

ion by solvent molecules is an indispensable factor for favoring the formation of glucose **7**.

For reactions in solution, it turns out that the separation of the two glucose units at **TS₃₄** requires the largest energy, while the subsequent water attack and deprotonation steps are energetically downhill. The slight exothermicity of the overall reaction highlights that the product **7** is significantly stabilized compared to the gas phase. Following numerous studies like Ref. [40], the reaction free energy from **1** to **7** in aqueous solution (ΔG_{reac}^{sol}) is evaluated by

$$\Delta G_{reac}^{sol} = \Delta G_{1\rightarrow 7}^{sol} - RT \ln[H_2O], \qquad (1)$$

where $\Delta G_{1\rightarrow 7}^{sol}$ is the computed Gibbs free energy change, R is a gas constant, T is a temperature, and $[H_2O]$ is a molar concentration of
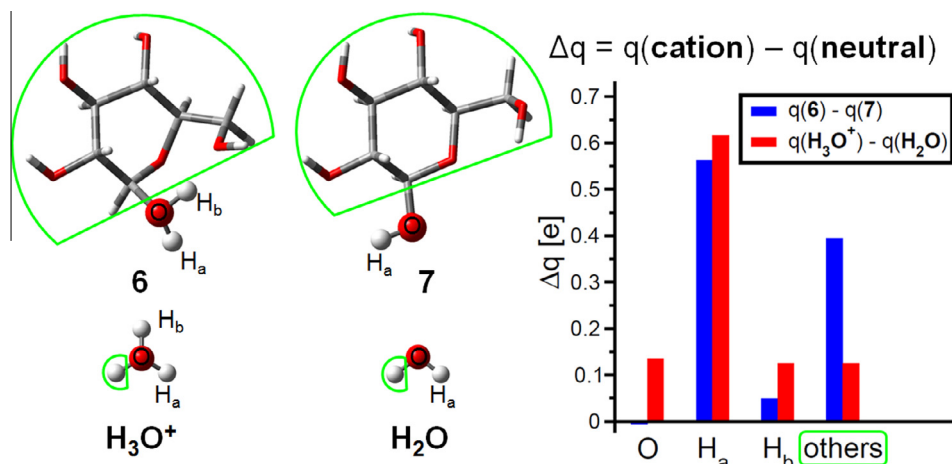

Figure 4. Left: Definition of atomic labels (O, H_a, H_b) for population analysis. The region surrounded by the green line is represented as 'others' in the plot on the right hand side. Right: Magnitude of delocalization of a positive charge (Δq) on each site. 'q' is the natural atomic charge calculated at the B3LYP/6-31+G(d) level in gas phase. (For interpretation of the references to colour in this figure legend, the reader is referred to the web version of this article.)

Table 1
Energy contributions of solvation effects [kcal/mol] at the RI-SCS-MP2/aug-cc-pVDZ//B3LYP/6-31+G(d) level of theory.

	E^{reorg}	$\Delta\mu$	Total
In water			
1 + H$_2$O	73.20	44.95	118.15
2 × **7**	67.99	36.29	104.28
(2 × **7**) – (**1 + H$_2$O**)	–5.21	–8.66	–13.87
In [mmim][Cl]			
1 + H$_2$O	81.89	51.53	133.42
2 × **7**	69.14	27.88	97.02
(2 × **7**) – (**1 + H$_2$O**)	–12.75	–23.65	–36.40

pure water (55.5 M). In this work, the value is −3.44 kcal/mol, which is consistent with the thermodynamic parameter experimentally obtained from an enzymatic hydrolysis reaction (⩽−3.0 kcal/mol) [41].

The barrier height at **TS$_{34}$** in [mmim][Cl] is 9.9 kcal/mol higher than that in the aqueous phase. To make a comparison with experimental results, the RISM-SCF-SEDD free energies were converted into activation energies where the entropic term was calculated by numerical differentiation of solvent temperature. Our theoretical values are 14.1 kcal/mol in water and 24.5 kcal/mol in [mmim][Cl], respectively. The result in [mmim][Cl] is in good agreement with the experimental value (26.5 ± 2.9 kcal/mol in [emim][Cl] [42], [emim]$^+$ denotes 1-Ethyl-3-methylimidazolium cation); nevertheless, we observe a qualitative difference from experimentally available data in water such as 26.4 ± 7.1 [43] and 32.3 kcal/mol [44]. The underestimation may be affected by ignoring the counteranion in the system, the existence of competing reaction pathways, and/or the level of theory.

3.3. Solvation free energy and solvation structure

Next we closer examine the nature of the primary factor for the large stabilization of **7** in solution. The focused free energy change $\Delta\Delta G^{\mathrm{sol}}_{1\to7}$ can be decomposed as follows:

$$\Delta\Delta G^{\mathrm{sol}}_{1\to7} = 2 \times \Delta G^{\mathrm{sol}}_{\mathbf{7}} - (\Delta G^{\mathrm{sol}}_{1} + \Delta G^{\mathrm{sol}}_{H_2O})$$
$$= \Delta\Delta E^{\mathrm{gas}}_{1\to7} + \Delta\Delta E^{\mathrm{therm}}_{1\to7} + 2 \times (E^{\mathrm{reorg}}_{7} + \Delta\mu_7)$$
$$- (E^{\mathrm{reorg}}_{1} + \Delta\mu_1 + E^{\mathrm{reorg}}_{H_2O} + \Delta\mu_{H_2O}) \quad (2)$$

where $\Delta\Delta E^{\mathrm{gas}}_{1\to7}$ is the corresponding electronic energy change in gas phase using optimized geometries in water (+6.33 kcal/mol) and in [mmim][Cl] (+12.23 kcal/mol). $\Delta\Delta E^{\mathrm{therm}}_{1\to7}$ denotes the thermal correction calculated in each solution. E^{reorg} is the energy contribution of solvation effects to the electronic structure of the solute molecule.

$$E^{\mathrm{reorg}} = \left\langle \Psi^{\mathrm{sol}} \middle| H \middle| \Psi^{\mathrm{sol}} \right\rangle - \left\langle \Psi^{\mathrm{gas}} \middle| H \middle| \Psi^{\mathrm{gas}} \right\rangle \quad (3)$$

In Eq. (3), $\left| \Psi^{\mathrm{sol}} \right\rangle$ and $\left| \Psi^{\mathrm{gas}} \right\rangle$ stand for wavefunctions in solution and gas phase. $\Delta\mu$ is the computed solvation free energy.

Table 1 summarizes these energy components for reactants and products. The calculated difference confirms that glucose **7** receives stabilization in both solvents, with the main contribution coming from $\Delta\mu$. The more than twice greater stabilization in [mmim][Cl] is remarkable.

Solvation free energy are formally given by the summation of the value from each atomic site α [24,45,46].

$$\Delta\mu = \sum_{\alpha}^{\mathrm{atom}} \Delta\mu_{\alpha} \quad (4)$$

Figure 5 shows the quantity defined as $\Delta\mu_{\alpha}$ in gas phase geometry subtracted from $\Delta\mu_{\alpha}$ in solution for **7**. This analysis clearly tells the strongly interacting atomic site with solvents. In the case of water, the labels O11 and O12 serve as the first two atomic sites with large stabilization (−7.35 and −6.46 kcal/mol, respectively). On the other hand, that role is played by H21 (−11.57 kcal/mol) and H23 (–8.73 kcal/mol) in [mmim][Cl]. The oxygen and hydrogen atoms connected with aforementioned labels work in opposite directions. In particular, the label O1 presents the most significant destabilization (+5.87 kcal/mol in water and +6.58 kcal/mol in [mmim][Cl]).

The radial distribution functions (RDFs) for interaction sites discussed above are plotted in Figure 6. For H21 and H23 labels, the peak of RDF of chloride anion in [mmim][Cl] located at 2.2 Å
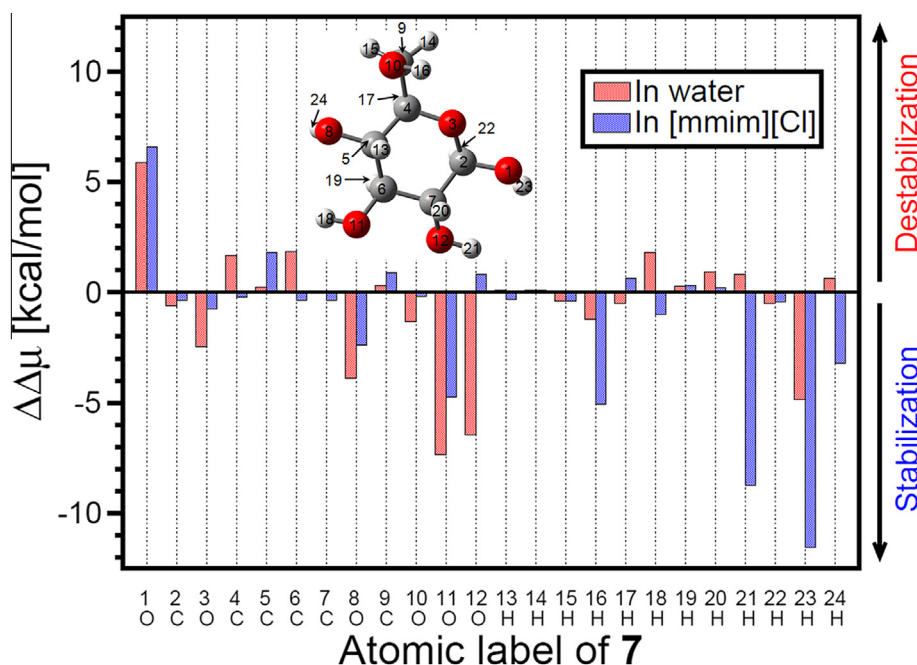

Figure 5. Difference of divided solvation free energy $\Delta\Delta\mu = \Delta\mu^{\mathrm{sol}}_{\alpha} - \Delta\mu^{\mathrm{gas}}_{\alpha}$ of **7** at RI-SCS-MP2/aug-cc-pVDZ//B3LYP/6-31+G(d) level. The definition of atomic labels is given in the inset.
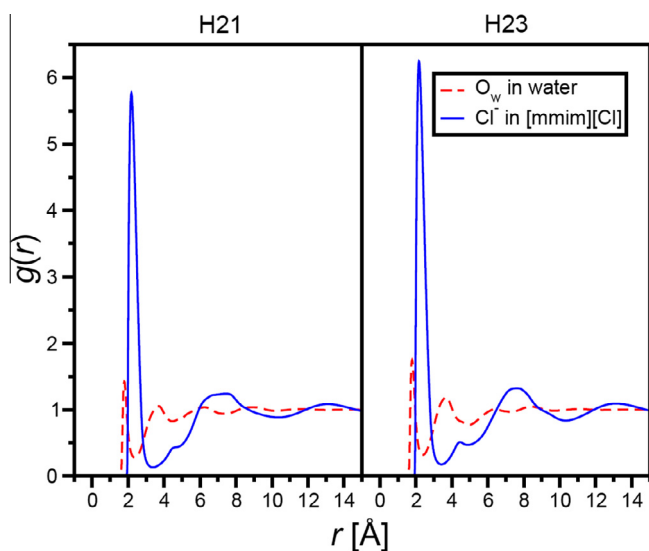
Figure 6. RDFs between hydrogens of **7** and electronegative solvent sites. See the inset in Figure 5 for specification of atomic labels.

becomes more than three times as intensive as the first peak of solvent oxygen (O_w) in aqueous solution around 1.8 Å. Since this peak is the counterpart of direct contact between hydrogen atomic site of solute and electronegative solvent site, the difference of solvation structure clarify the increasing of attractive interactions in [mmim][Cl] in Figure 5. The RDFs of Cl^-–H at 3.0–6.0 Å region are fairly small, reflecting that [mmim]$^+$ cations exist in the vicinity of chloride anions. Even though the shape of RDF in aqueous solution expects solvent water molecules do not contribute to the dramatic stabilization of **7**, we should keep in mind that a presence of counteranion is omitted in this work. It would be another source for stabilization if the counteranion approaches electropositive interaction sites.

In short, the strong interaction of OH groups with solvent molecules makes the glucose stable in solution and [mmim][Cl] performs better than water in its stabilization in terms of solvation free energy and solvation structure.

4. Conclusion

The reaction free energy profiles of S_N1-type cellobiose hydrolysis reaction to glucose have been determined in gas phase, in aqueous solution, and in [mmim][Cl], where the RISM-SCF-SEDD method was successfully employed to describe solvation effects. In solution, the reaction barrier is assigned to the dissociation of the glycosidic bond and the calculated activation energy at the RI-SCS-MP2//aug-cc-pVDZ//B3LYP/6-31+G(d) level of theory in [mmim][Cl] (24.5 kcal/mol) is comparable with the experimental data (26.5 kcal/mol in [42]). The calculated activation energy in water (14.1 kcal/mol) is lower than in the experiment (26.4 kcal/mol [43]). It is probably desirable to revisit energetics in a future study, using highly sophisticated methods (for example, coupled cluster singles, doubles, and perturbative triples (CCSD(T))) together with sufficiently large basis sets, and possibly most importantly, including the counteranion in the system. Decomposition of the solvation free energy and the solvation structure bring the important insight that the interaction of hydroxyl groups with solvent molecules is attributed to the stabilization of the glucose reaction product. Notably, a huge enhancement of the first peak in RDFs indicates that chloride anions in [mmim][Cl] strongly interact with hydroxyl-group hydrogen interaction sites. Our group plans next to establish the hydrolysis mechanism of glucose to fructose and hydroxymethylfurfural (HMF) in an acidic environment and in ILs. In the future,

we would like to take how the hydrolysis process is influenced by using different cation components of ILs into consideration, which is systematically examined in recent experimental study [35].

Appendix A. Supplementary data

Supplementary data associated with this article can be found, in the online version, at http://dx.doi.org/10.1016/j.cplett.2014.04.014.

References

[1] J.D. Peterson, L.O. Ingram, Ann. N.Y. Acad. Sci. 1125 (2008) 363.
[2] R.W. Torget, J.S. Kim, Y.Y. Lee, Ind. Eng. Chem. Res. 39 (2000) 2817.
[3] J.F. Saeman, Ind. Eng. Chem. 37 (1945) 43.
[4] R.P. Swatloski, S.K. Spear, J.D. Holbrey, R.D. Rogers, J. Am. Chem. Soc. 124 (2002) 4974.
[5] C. Li, Z.K. Zhao, Adv. Synth. Catal. 349 (2007) 1847.
[6] Y. Zhang, H. Du, X. Qian, E.Y.-X. Chen, Energy Fuels 24 (2010) 2410.
[7] H. Zhao, J.E. Holladay, H. Brown, Z.C. Zhang, Science 316 (2007) 1597.
[8] Y. Su et al., Appl. Catal. A 391 (2011) 436.
[9] J.M. Stubbs, D. Marx, Chem. Eur. J. 11 (2005) 2651.
[10] X. Qian, M.R. Nimlos, M. Davis, D.K. Johnson, M.E. Himmel, Carbohydr. Res. 340 (2005) 2319.
[11] H. Dong, M.R. Nimlos, M.E. Himmel, D.K. Johnson, X. Qian, J. Phys. Chem. A 113 (2009) 8577.
[12] X. Liang, A. Montoya, B.S. Haynes, J. Phys. Chem. B 115 (2011) 10682.
[13] H. Liu, K.L. Sale, B.M. Holmes, B.A. Simmons, S. Singh, J. Phys. Chem. B 114 (2010) 4293.
[14] K. Kitaura, E. Ikeo, T. Asada, T. Nakano, M. Uebayasi, Chem. Phys. Lett. 313 (1999) 701.
[15] M.S. Gordon, J.M. Mullin, S.R. Pruitt, L.B. Roskop, L.V. Slipchenko, J.A. Boatz, J. Phys. Chem. B 113 (2009) 9646.
[16] E.I. Izgorodina, J. Rigby, D.R. MacFarlane, Chem. Commun. 48 (2012) 1493.
[17] D. Yokogawa, H. Sato, S. Sakaki, J. Chem. Phys. 126 (2007) 244504.
[18] D. Yokogawa, H. Sato, S. Sakaki, J. Chem. Phys. 131 (2009) 214504.
[19] D. Chandler, H.C. Andersen, J. Chem. Phys. 57 (1972) 1930.
[20] F. Hirata, P.J. Rossky, Chem. Phys. Lett. 83 (1981) 329.
[21] S. Ten-no, F. Hirata, S. Kato, Chem. Phys. Lett. 214 (1993) 391.
[22] H. Sato, F. Hirata, S. Kato, J. Chem. Phys. 105 (1996) 1546.
[23] S. Hayaki, K. Kido, D. Yokogawa, H. Sato, S. Sakaki, J. Phys. Chem. B 113 (2009) 8227.
[24] S. Hayaki, K. Kido, H. Sato, S. Sakaki, Phys. Chem. Chem. Phys. 12 (2010) 1822.
[25] A.D. Becke, J. Chem. Phys. 98 (1993) 5648.
[26] C. Lee, W. Yang, R.G. Parr, Phys. Rev. B 37 (1988) 785.
[27] W.J. Hehre, R. Ditchfield, J.A. Pople, J. Chem. Phys. 56 (1972) 2257.
[28] P.C. Hariharan, J.A. Pople, Theor. Chem. Acc. 28 (1973) 213.
[29] T. Clark, J. Chandrasekhar, G.W. Spitznagel, P.v.R. Schleyer, J. Comput. Chem. 4 (1983) 294.
[30] S. Grimme, J. Chem. Phys. 118 (2003) 9095.
[31] M. Feyereisen, G. Fitzgerald, A. Komornicki, Chem. Phys. Lett. 208 (1993) 359.
[32] M. Katouda, S. Nagase, Int. J. Quant. Chem. 109 (2009) 2121.
[33] T.H. Dunning Jr., J. Chem. Phys. 90 (1989) 1007.
[34] R.A. Kendall, T.H. Dunning Jr., R.J. Harrison, J. Chem. Phys. 96 (1992) 6796.
[35] B. Lu, A. Xu, J. Wang, Green Chem. 16 (2014) 1326.
[36] A. Kovalenko, F. Hirata, J. Chem. Phys. 110 (1999) 10095.
[37] Gaussian 09, Revision B.1, M.J. Frisch et al., Gaussian Inc, Wallingford CT, 2009.
[38] M.W. Schmidt et al., J. Comput. Chem. 14 (1993) 1347.
[39] K.B. Wiberg, Tetrahedron 24 (1968) 1083.
[40] D. Yokogawa, K. Ono, H. Sato, S. Sakaki, Dalton Trans. 40 (2011) 11125.
[41] Y.B. Tewari, R.N. Goldberg, J. Biol. Chem. 264 (1989) 3966.
[42] L. Vanoye, M. Fanselow, J.D. Holbrey, M.P. Atkins, K.R. Seddon, Green Chem. 11 (2009) 390.
[43] N.S. Mosier, C.M. Ladisch, M.R. Ladisch, Biotechnol. Bioeng. 79 (2002) 610.
[44] J.-H.Q. Pinto, S. Kaliaguine, AIChE J. 37 (1991) 905.
[45] H. Sato, F. Hirata, J. Mol. Struct. (THEOCHEM) 461–462 (1999) 113.
[46] S. Hayaki, D. Yokogawa, H. Sato, S. Sakaki, Chem. Phys. Lett. 458 (2008) 329.